

Design of a Trajectory Tracking Controller for Coreless Tubular Linear Motor Using Model Predictive Controller

Nguyen Trung Thanh^{1*} , Nguyen Minh Cuong² , Dang Danh Hoang³ , Le Thi Thuy Ngan⁴ 

DOI:DOI:10.5281/zenodo.15104520

^{1*} Nguyen Trung Thanh, Faculty of Mechanical Electrical, Electronics Technology, Thai Nguyen University of Technology, Vietnam.


² Nguyen Minh Cuong, Faculty of Electrical Engineering, Thai Nguyen University of Technology, Vietnam.

³ Dang Danh Hoang, Faculty of Mechanical Electrical, Electronics Technology, Thai Nguyen University of Technology, Vietnam.

⁴ Le Thi Thuy Ngan, Faculty of Mechanical Electrical, Electronics Technology, Thai Nguyen University of Technology, Vietnam.

This paper presents a cascaded control structure for a coreless tubular linear motor. The system includes position and speed loops employing PI controllers, and a current loop using Finite Control Set Model Predictive Control (FCS-MPC). This structure addresses challenges associated with low stator inductance, specifically its impact on current control. A simulation model was developed using MATLAB/Simulink. The simulation results demonstrate the effectiveness of the proposed solution in tracking the desired trajectory and minimizing the negative effects of low stator inductance on the current loop.

Keywords: FCS-MPC, Tubular linear motor, coreless linear Motor

Corresponding Author	How to Cite this Article	To Browse
<p>Nguyen Trung Thanh, Faculty of Mechanical Electrical, Electronics Technology, Thai Nguyen University of Technology, , Vietnam.</p> <p>Email: nguyentrongthanh@tnut.edu.vn</p>	<p>Nguyen Trung Thanh, Nguyen Minh Cuong, Dang Danh Hoang, Le Thi Thuy Ngan, Design of a Trajectory Tracking Controller for Coreless Tubular Linear Motor Using Model Predictive Controller. Appl. Sci. Eng. J. Adv. Res.. 2025;4(2):1-7.</p> <p>Available From</p> <p>https://asejar.singhpublication.com/index.php/ojs/article/view/131</p>	

Manuscript Received 2025-02-03	Review Round 1 2025-02-24	Review Round 2	Review Round 3	Accepted 2025-03-17
Conflict of Interest None	Funding Nil	Ethical Approval Yes	Plagiarism X-checker 3.44	Note



© 2025 by Nguyen Trung Thanh, Nguyen Minh Cuong, Dang Danh Hoang, Le Thi Thuy Ngan and Published by Singh Publication. This is an Open Access article licensed under a Creative Commons Attribution 4.0 International License <https://creativecommons.org/licenses/by/4.0/> unported [CC BY 4.0].



1. Introduction

The applications of linear motors are becoming increasingly widespread in both industrial and domestic settings. These applications include industrial automation, transportation, renewable energy, and more [1-3]. The advantage of linear motors lies in their ability to provide direct thrust without the need for complex mechanical structures [4-6]. As a result, they are highly suitable for applications requiring high reliability, high efficiency, and compact dimensions. There are various types of linear motor based on their configurations. These configurations include flat single-sided, flat double-sided, and tubular structures [7, 8]. However, they share a common feature: the stator windings surround the rotor, which is composed of permanent magnets. In the tubular structure, the stator consists of disk-shaped coils arranged coaxially, while the rotor is formed by cylindrical magnets sequentially placed within a circular tubular housing (Figure 1).

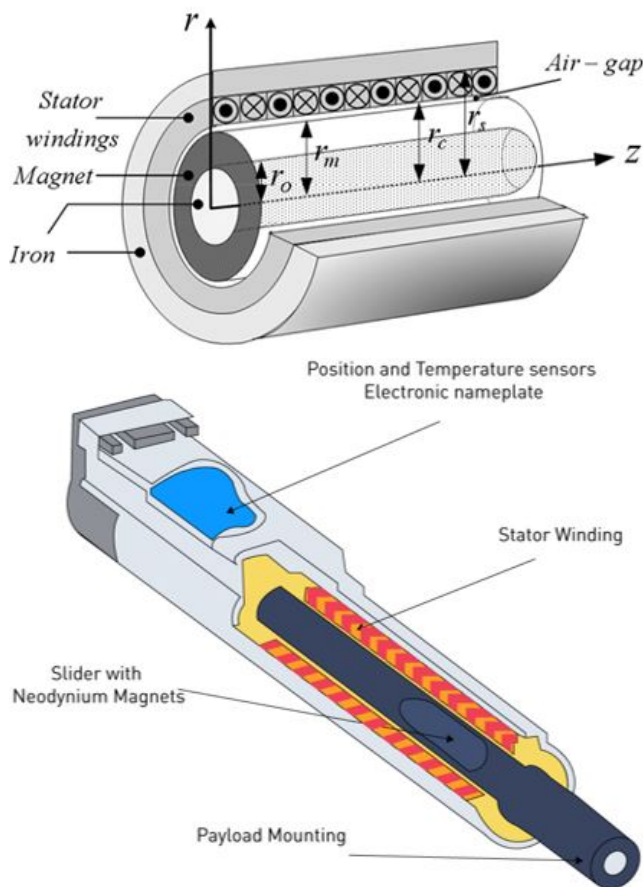


Figure 1: Structure of a Tubular Linear Motor [8]

Tubular linear motors can be constructed with or without an iron core [9, 10].

However, tubular linear motors are predominantly manufactured without an iron core. The absence of an iron core in the stator results in low stator inductance and causes thrust force ripple [11]. Although PID controllers are effectively applied to rotary motors [12, 13], traditional methods still have limitations, such as not considering control signal constraints, state constraints, the impact of load disturbances, and variations in system inertia [14].

For coreless tubular linear motors, the rotor shaft is more sensitive to load disturbances due to the lack of intermediate transmission mechanisms. PID controllers also often produce large, undesirable overshoots. The current loop is the primary cause of this problem. To address these issues, modern controllers have been applied, such as sliding mode controllers [15, 16], fuzzy controllers [17, 18], and adaptive controllers using neural networks [19-21]. However, these solutions often overlook the limitations of the power converter. Meanwhile, the power converter has only a limited ability to provide energy responses.

A control structure is proposed, employing PI controllers for the speed and position loops and Finite Control Set Model Predictive Control (FCS-MPC) for the current loop. The design of these controllers, considering input constraints, is presented in Section 2. A simulation in MATLAB/Simulink is then used to evaluate the performance of the proposed solution.

2. Control Design

a. Discretized model of the coreless tubular linear motor

The mathematical model of the tubular linear motor is described based on the principles of electromagnetism. Based on this, an approach to modeling the mathematical system in the dq coordinate frame is established, as presented in reference [22].

$$\begin{cases} \frac{di_d}{dt} = \frac{u_d}{L_s} - \frac{R_s}{L_s} i_d + \omega_r i_q \\ \frac{di_q}{dt} = \frac{u_q}{L_s} - \frac{R_s}{L_s} i_q - \omega_r i_d - \frac{\omega_r}{L_s} \psi_f \end{cases} \quad (1)$$

Where: i_d and i_q are the currents on the d-axis and q-axis,

respectively; u_d and u_q are the output voltages of the converter on the d-axis and q-axis, respectively. ψ_f is the magnetic flux generated by the permanent magnets of the rotor; ω_r is the angular velocity converted from the linear velocity of the motor and is determined by the following expression:

$$\omega_r = \frac{\pi}{\tau} v \text{ where } v \text{ is the linear velocity of the rotor.}$$

And the thrust force is determined by the expression:

$$F_T = \frac{3}{2} \frac{\pi p}{\tau} k_F (\psi_d i_q - \psi_q i_d) \quad (2)$$

where p is the number of pole pairs of the motor, ψ_d, ψ_q are the magnetic fluxes generated by the permanent magnets on the d-axis and q-axis, respectively.

To facilitate the design of the controller, we choose the d-axis to align with the magnetic flux axis of the rotor's permanent magnets. Therefore, the thrust force expression can be rewritten as follows:

$$F_T = \frac{3}{2} \frac{\pi p}{\tau} k_F \psi_f i_q \quad (3)$$

Applying Newton's second law to the motor, we obtain the dynamic equation of the motor:

$$\begin{cases} \frac{dx}{dt} = v \\ \frac{dv}{dt} = \frac{1}{m} (F_T - F_L) \end{cases} \quad (4)$$

From(1) ,(3) and(4) , the motor model can be rewritten in matrix form as:

$$\frac{di_{dq}}{dt} = \mathbf{T} \mathbf{i}_{dq} + \mathbf{L} \mathbf{u}_{dq} + \mathbf{W} \mathbf{i}_{dq} \omega_r + \mathbf{P} \psi_f \omega_r \quad (5)$$

$$\text{where } \mathbf{i}_{dq} = [i_d \ i_q]^T; \mathbf{i}_{qd} = [i_q \ i_d]^T; \mathbf{T} = \begin{bmatrix} R_s \\ L_s \end{bmatrix}; \mathbf{L} = \begin{bmatrix} 1 \\ L_s \end{bmatrix}; \mathbf{W} = \begin{bmatrix} 0 & 1 \\ -1 & 0 \end{bmatrix}; \mathbf{P} = \begin{bmatrix} 0 \\ -1/L_s \end{bmatrix}$$

Equations and form the basis for designing the position, speed, and current controllers in the following section.

b. Outer-loop controller design

Based on the system of equations(4) , a cascaded two-loop control structure is designed. The equations presented in can be expressed in the following transfer function form:

$$\begin{cases} G_x(s) = \frac{X(s)}{V(s)} = \frac{1}{s} \\ G_v(s) = \frac{V(s)}{I_q(s)} = \frac{3}{2} k_F \psi_f \frac{\pi p}{\tau m s} \end{cases} \quad (6)$$

The plant for each controller is considered to be an integrator; therefore, a PI controller can be chosen with the following form:

$$u(s) = K_p \left(1 + \frac{1}{T_s} \right) e(s) \quad (7)$$

Applying the pole placement method with the desired specifications, the controller parameters for the position loop and speed loop are obtained.

c. Inter-loop controller design

To design the current controller, the motor description equation(5) is discretized with a sampling time T_s as follows:

$$\mathbf{i}_{dq}(k+1) = \mathbf{i}_{dq}(k) + \mathbf{T}_s \mathbf{i}_{dq}(k) + \mathbf{L}_s \mathbf{u}_{dq}(k) + \mathbf{W}_s \mathbf{i}_{dq}(k) \omega_r(k) + \mathbf{P}_s \psi_f \omega_r(k) \quad (8)$$

Where $\mathbf{T}_s = T_s \begin{bmatrix} \frac{R_s}{L_s} \\ 1 \end{bmatrix}$; $\mathbf{L}_s = T_s \begin{bmatrix} 1 \\ L_s \end{bmatrix}$; $\mathbf{W}_s = T_s \begin{bmatrix} 0 & 1 \\ -1 & 0 \end{bmatrix}$; $\mathbf{P}_s = T_s \begin{bmatrix} 0 \\ -1/L_s \end{bmatrix}$

With T_s being the sampling time of the current, typically equal to the carrier frequency of the converter, from the discretized model(8) , we can rewrite it as follows:

$$\begin{aligned} \mathbf{i}_{dq}(k+1) &= \mathbf{i}_{dq}(k) + \mathbf{T}_s \mathbf{i}_{dq}(k) + \mathbf{W}_s \mathbf{i}_{dq}(k) \omega_r(k) + \mathbf{L}_s \mathbf{u}_{dq}(k) + \mathbf{P}_s \psi_f \omega_r(k) = \\ &= \mathbf{\Phi} \mathbf{i}_{dq}(k) + \mathbf{L}_s \mathbf{u}_{dq}(k) + \mathbf{P}_s \psi_f \omega_r(k) \end{aligned} \quad (9)$$

Where $\mathbf{\Phi} = \mathbf{I} + \mathbf{T}_s + \mathbf{W}_s \omega_r(k)$

Based on the discretized model (9), a current prediction model is constructed as follows:

$$\mathbf{i}_{dq}^{est}(k+i+1|k) = \mathbf{\Phi} \mathbf{i}_{dq}^{est}(k+i|k) + \mathbf{L}_s \bar{\mathbf{u}}_{dq}(k) + \mathbf{P}_s \psi_f \omega_r(k) \quad (10)$$

Where $\mathbf{i}_{dq}^{est} = \mathbf{i}_{dq}(k)$ is the current at the k -th sampling time; $\bar{\mathbf{u}}_{dq}(k+i)$ is the control signal for the next i -th step, with the prediction horizon N . The goal of the controller is to find an optimal control value. We select the value function in the following quadratic form:

$$J = \sum_{i=1}^N \left[\left(\mathbf{i}_{dq}^{ref} - \mathbf{i}_{dq}^{est}(k+i) \right) \mathbf{Q} \left(\mathbf{i}_{dq}^{ref} - \mathbf{i}_{dq}^{est}(k+i) \right) \right] \quad (11)$$

Where $\mathbf{Q} = \begin{bmatrix} \lambda & 0 \\ 0 & 1 \end{bmatrix}$ is a positive definite diagonal matrix, the coefficient λ_d is the weighting factor of the deviation in the value function J . \mathbf{i}_{dq}^{ref}

is the output of the outer-loop controller.

The control signal is \mathbf{u}_{dq} generated by a three-phase inverter. This converter uses the SVM modulation method based on 6 basic vectors. With this method, the modulation values are normalized to form the vector $\mathbf{u}_s = [u_a \ u_b \ u_c]^T$. Therefore, a finite number of voltage vectors can be applied to the motor. In this paper, six fundamental vectors and six vectors created by pulse-width modulating the fundamental vectors to half their magnitude are used to form the vector set $\mathbf{U} = \{\mathbf{u}_0, \mathbf{T}\mathbf{u}_1, \mathbf{T}\mathbf{u}_2, \dots, \mathbf{T}\mathbf{u}_{11}, \mathbf{T}\mathbf{u}_{12}\}$, as shown in Fig. 3.

The minimization of (11) can be achieved by sequentially replacing each voltage vector in Table 1 to find the optimal control signal. This approach helps reduce the computation time of the system, enabling a quick response to changes in load disturbances.

To reduce the computation time, the prediction horizon is limited to $N=2$. Substituting equation(10) into equation (11), the condition for the control signal is obtained as follows:

$$\begin{aligned} \min_{\bar{\mathbf{u}}_{dq}(k), \bar{\mathbf{u}}_{dq}(k+1)} J &= \bar{\mathbf{u}}_{dq}^T(k) \mathbf{H}^T \mathbf{Q} \mathbf{H} \bar{\mathbf{u}}_{dq}(k) + \bar{\mathbf{u}}_{dq}^T(k+1) \mathbf{H}^T \mathbf{Q} \mathbf{H} \bar{\mathbf{u}}_{dq}(k+1) + \bar{\mathbf{u}}_{dq}^T(k) \mathbf{H}^T \mathbf{Q} \mathbf{H} \bar{\mathbf{u}}_{dq}(k+1) + \\ &+ 2 \left(\mathbf{\Phi} \mathbf{i}_{dq}(k) + \mathbf{h} \psi_f - \mathbf{i}_{dq}^{ref} \right)^T \mathbf{Q} \mathbf{H} \bar{\mathbf{u}}_{dq}(k) + 2 \left(\mathbf{\Phi}^2 \mathbf{i}_{dq}(k) + \mathbf{\Phi} \mathbf{h} \psi_f - \mathbf{i}_{dq}^{ref} \right)^T \mathbf{Q} \mathbf{H} \bar{\mathbf{u}}_{dq}(k+1) \end{aligned}$$

With $\bar{\mathbf{u}}_{dq} \in \mathbf{U} = \{\mathbf{u}_0, \mathbf{T}\mathbf{u}_1, \mathbf{T}\mathbf{u}_2, \dots, \mathbf{T}\mathbf{u}_{11}, \mathbf{T}\mathbf{u}_{12}\}$ (12)

$$\text{Where } \mathbf{T} = \begin{bmatrix} \cos(\theta) & -\sin(\theta) \\ \cos(\theta - \frac{2\pi}{3}) & -\sin(\theta - \frac{2\pi}{3}) \\ \cos(\theta + \frac{2\pi}{3}) & -\sin(\theta + \frac{2\pi}{3}) \end{bmatrix}$$

Expression (12) represents the condition for determining the control signal u_{dq} for the current loop. By applying minimization algorithms to solve the system of equations (12), we obtain the desired optimal control signal.

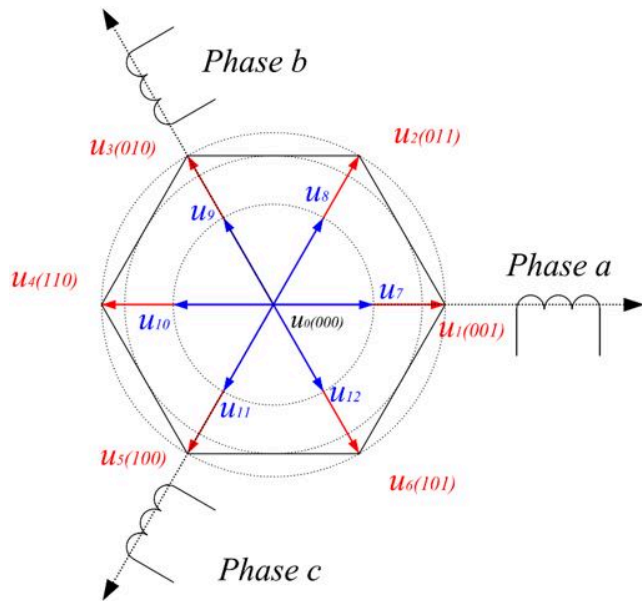


Figure 2: The voltage vectors \mathbf{U}

3. Simulation Results

To validate the controllers obtained by minimizing the objective functions in(12), a simulation model was developed using Matlab/Simulink software, with the motor parameters provided in Table 1.

Table 1. Motor parameters

Motor parameters	Symbol	Value	Unit
d-axis stator inductance	Lsd	1.4	mH
q-axis stator inductance	Lsq	1.4	mH
Stator resistance	Rs	10.3	Ω
Rotor flux	ψ_p	0.035	Wb
Number of pole pairs	zp	2	
Pole step	tp	0.02	m

A simulation scenario was designed to test the response capability of the entire system. A straight-line trajectory was used for this purpose. To ensure the differentiability of the trajectory, the set speed was kept constant during the motor's movement. Specifically, the motor moves from the position 0mm to 80mm in 0.5s with a speed of 160mm/s and maintains the position for 1s. After that,

the motor moves back to the 0mm position in 0.5s with a speed of 160mm/s. At $t=1s$, a load force $F_L=5N$ is applied.

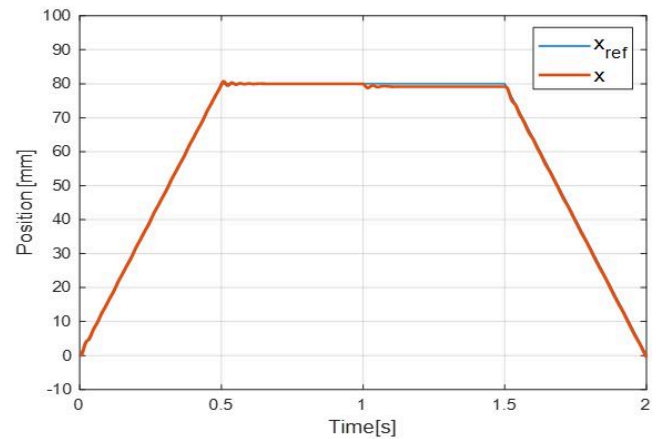


Figure 3: The position response of the motor

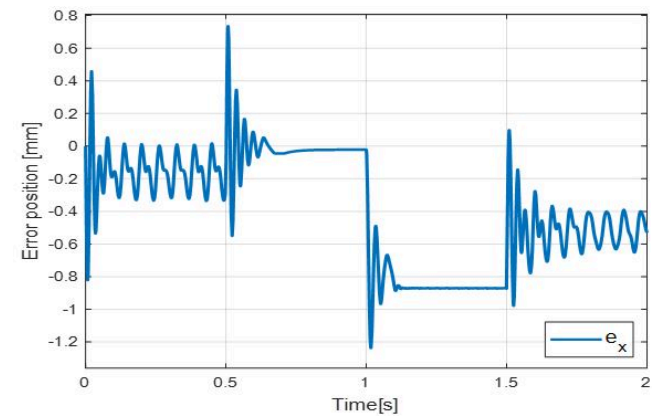


Figure 4: The error position of the motor.

The trajectory and response of the motor are shown in Figure 3, demonstrating the ability to track the reference trajectory. The position error of the motor relative to the trajectory, with $e_{x\max}=0.8\text{mm}$, meets the specified quality criteria.

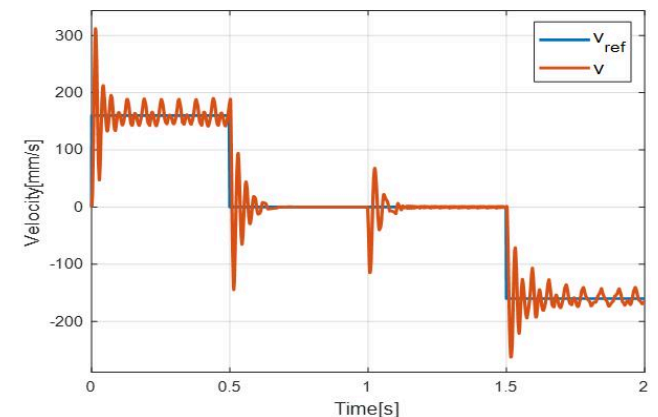


Figure 5: The speed response of the motor.

Meanwhile, the motor speed tracks the set speed during the motor's movement.

However, speed fluctuations during movement are caused by limited number of current vectors used in inner-loop controller, as shown in Figures 5.

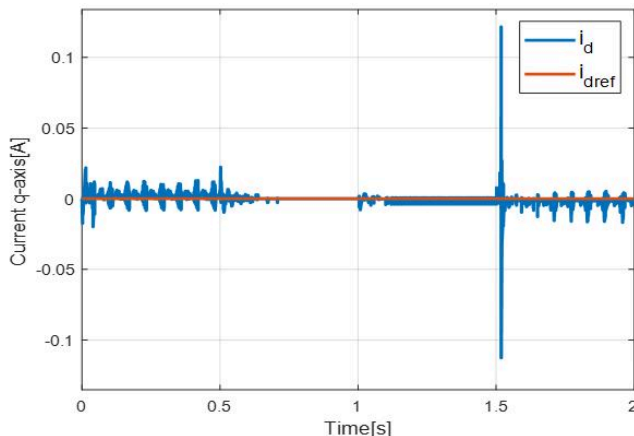


Figure 6:Response of current id

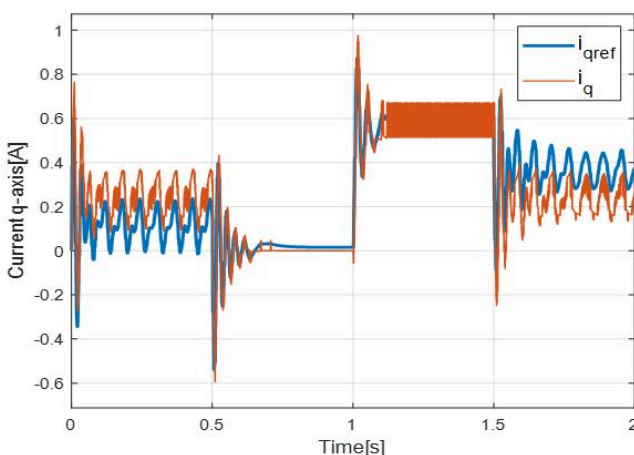


Figure 7:Response of current iq

In order to reduce computational load, prediction horizon and number of voltage vectors used are limited. In simulation results with a prediction horizon of $N = 2$ and number of voltage vectors used $n = 13$, results in Figures 6 and 7 demonstrate rapid response capability of current controller to changes in reference value.

4. Conclusion

This paper presents a proposed control structure with two control loops: speed and position loop, and current loop. In this structure, outer loop is designed using a PI controller to stability position and velocity. Meanwhile, inner loop (current loop) is designed using FCS-MPC controller to respond quickly to changes in current under low stator inductance conditions. Simulation results demonstrate that combination of two loops significantly improves overall system response.

In particular, it overcomes the fundamental drawback of traditional PID controllers.

ACKNOWLEDGMENT

The authors gratefully acknowledge Thai Nguyen University of Technology, Vietnam, for supporting this work.

References

- Wakiwaka, H. (2024). Magnetic application in linear motor. In *Handbook of Magnetic Material for Motor Drive Systems* (pp. 1-16). Singapore: Springer Nature Singapore. https://doi.org/10.1007/978-981-19-9644-3_54-1
- Gang, L. Y. U. (2020). Review of the application and key technology in the linear motor for the rail transit. *Proceedings of the CSEE*, 40(17), 5665-5675. DOI:10.13334/j.0258-8013.pcsee.200488
- Jansen, J. W., Smeets, J. P. C., Overboom, T. T., Rovers, J. M. M., & Lomonova, E. A. (2014). Overview of analytical models for the design of linear and planar motors. *IEEE Transactions on Magnetics*, 50(11), 1-7. DOI:10.1109/TMAG.2014.2328556
- Boldea, I., Tutelea, L. N., Xu, W., & Pucci, M. (2017). Linear electric machines, drives, and MAGLEVs: An overview. *IEEE Transactions on Industrial Electronics*, 65(9), 7504-7515. DOI:10.1109/TIE.2017.2733492
- Shahid, M. B., Jin, W., Abbasi, M. A., Husain, A. R. B., Munir, H. M., Hassan, M., ... & Alghamdi, T. A. (2024). Model predictive control for energy efficient AC motor drives: An overview. *IET Electric Power Applications*, 18(12), 1894-1920. <https://doi.org/10.1049/elp2.12517>
- Boldea, I. (2017). Electric generators and motors: An overview. *CES Transactions on Electrical Machines and Systems*, 1(1), 3-14. DOI:10.23919/TEMS.2017.7911104
- Gieras, J. F., Piech, Z. J., & Tomczuk, B. (2018). *Linear synchronous motors: transportation and automation systems*. CRC press. <https://doi.org/10.3390/en14092549>
- Jang, S. M., Choi, J. Y., Cho, H. W., & Lee, S. H. (2005). Thrust analysis and measurements of tubular linear actuator with cylindrical halbach array. *IEEE Transactions on magnetics*, 41(5), 2028-2031. DOI:10.1109/TMAG.2005.846266

9. Abdalla, I. I., Ibrahim, T., & Nor, N. M. (2018). Analysis of tubular linear motors for different shapes of magnets. *Ieee Access*, 6, 10297-10310. **DOI:**10.1109/ACCESS.2017.2775863
 10. Bianchi, N., Bolognani, S., Corte, D. D., & Tonel, F. (2003). Tubular linear permanent magnet motors: An overall comparison. *IEEE transactions on industry applications*, 39(2), 466-475. **DOI:**10.1109/TIA.2003.809444
 11. Leandro, M., Bianchi, N., Molinas, M., & Ummaneni, R. B. (2019, May). Low inductance effects on electric drives using slotless permanent magnet motors: A framework for performance analysis. In *2019 IEEE International Electric Machines & Drives Conference (IEMDC)* (pp. 1099-1105). IEEE. **DOI:**10.1109/IEMDC.2019.8785241
 12. Kang, G., & Nam, K. (2005). Field-oriented control scheme for linear induction motor with the end effect. *IEE Proceedings-Electric Power Applications*, 152(6), 1565-1572. <https://doi.org/10.1049/ip-epa:20045185>
 13. Cui, L., Zhang, H., & Jiang, D. (2019). Research on high efficiency V/f control of segment winding permanent magnet linear synchronous motor. *IEEE Access*, 7, 138904-138914. **DOI:**10.1109/ACCESS.2019.2930047
 14. Atencia, J., Martinez-Iturralde, M., Martinez, G., Rico, A. G., & Florez, J. (2003, June). Control strategies for positioning of linear induction motor: tests and discussion. In *IEEE International Electric Machines and Drives Conference, 2003. IEMDC'03.* (Vol. 3, pp. 1651-1655). IEEE. **DOI:**10.1109/IEMDC.2003.1210673
 15. Yu, L., Huang, J., Luo, W., Chang, S., Sun, H., & Tian, H. *Sliding-mode control for PMLSM position control—A review. Actuators* 12, 31 (2023). <https://doi.org/10.3390/act12010031>
 16. Shao, K., Zheng, J., Wang, H., Wang, X., Lu, R., & Man, Z. (2021). Tracking control of a linear motor positioner based on barrier function adaptive sliding mode. *IEEE Transactions on Industrial Informatics*, 17(11), 7479-7488. **DOI:**10.1109/TII.2021.3057832
 17. Liu, X., Wu, Q., Zhen, S., Zhao, H., Li, C., & Chen, Y. H. (2022). Robust constraint-following control for permanent magnet linear motor with optimal design: A fuzzy approach. *Information Sciences*, 600, 362-376. <https://doi.org/10.1016/j.ins.2022.03.083>
 18. Luo, M., Duan, J. A., & Yi, Z. (2023). Speed tracking performance for a coreless linear motor servo system based on a fitted adaptive fuzzy controller. *Energies*, 16(3), 1259. <https://doi.org/10.3390/en16031259>
 19. Liu, Z., Gao, H., Yu, X., Lin, W., Qiu, J., Rodríguez-Andina, J. J., & Qu, D. (2023). B-spline wavelet neural-network-based adaptive control for linear-motor-driven systems via a novel gradient descent algorithm. *IEEE Transactions on Industrial Electronics*, 71(2), 1896-1905. **DOI:**10.1109/TIE.2023.3260318
 20. Wang, Z., Hu, C., Zhu, Y., He, S., Yang, K., & Zhang, M. (2017). Neural network learning adaptive robust control of an industrial linear motor-driven stage with disturbance rejection ability. *IEEE Transactions on Industrial Informatics*, 13(5), 2172-2183. **DOI:**10.1109/TII.2017.2684820
 21. Ding, R., Ding, C., Xu, Y., & Yang, X. (2022). Neural-network-based adaptive robust precision motion control of linear motors with asymptotic tracking performance. *Nonlinear Dynamics*, 108(2), 1339-1356. <https://doi.org/10.1007/s11071-022-07258-0>
 22. Cheema, M. A. M., & Fletcher, J. E. (2020). *Advanced direct thrust force control of linear permanent magnet synchronous motor*. Springer International Publishing. <https://doi.org/10.1007/978-3-030-40325-6>
- Disclaimer / Publisher's Note: The statements, opinions and data contained in all publications are solely those of the individual author(s) and contributor(s) and not of Journals and/or the editor(s). Journals and/or the editor(s) disclaim responsibility for any injury to people or property resulting from any ideas, methods, instructions or products referred to in the content.